

*Research Article*

## **The Effect of Gaussian Blurring on the Extraction of Peaks and Pits from Digital Elevation Models**

A. Pathmanabhan and S. Dinesh

Received 27 December 2005; Revised 27 November 2006; Accepted 28 November 2006

Gaussian blurring is an isotropic smoothing operator that is used to remove noise and detail from images. In this paper, the effect of Gaussian blurring on the extraction of peaks and pits from digital elevation models (DEMs) is studied. First, a mathematical morphological-based algorithm to extract peaks and pits from DEMs is developed. Gaussian blurring is then implemented on the global digital elevation model (GTOPO30) of Great Basin using Gaussian kernels of different sizes and standard deviation values. The number of peaks and pits extracted from the resultant DEMs is computed using connected component labeling and the results are compared. The application of Gaussian blurring to perform the treatment of spurious peaks and pits in DEMs is also discussed. This work is aimed at studying the capabilities of Gaussian blurring in the modeling of objects and processes operating within an environment.

Copyright © 2007 A. Pathmanabhan and S. Dinesh. This is an open access article distributed under the Creative Commons Attribution License, which permits unrestricted use, distribution, and reproduction in any medium, provided the original work is properly cited.

### **1. Introduction**

A digital elevation model (DEM) is a set of points defined in a three-dimensional Cartesian space ( $X$ ,  $Y$ ,  $Z$ ) that approximates a topographic surface. The  $X$ - and  $Y$ -axes are an approximation of geographic coordinates (i.e., longitude and latitude), whereas the  $Z$ -axis represents the altitude above sea level. It is a digital file consisting of the terrain elevations for ground positions at regularly spaced horizontal intervals. DEMs can be generated directly through photogrammetric processing of stereo photos or satellite imagery such as stereoscopic SPOT images, or indirectly from the interpolation of scattered point elevation data, of contour lines, or of triangular irregular networks (TINs). DEMs are essential for many aspects of terrain and environmental modeling because of their

simple data structure and widespread availability, and they lend themselves to many GIS processes and operations [1].

The peaks of a terrain refer to the highest points of the mountains of the terrain while the pits of the terrain are the lowest points of the basins of the terrain. In DEMs, peaks are connected components that are completely surrounded by pixels of lower elevation while pits are connected components that are completely surrounded by pixels of higher elevation. The extraction of peaks and pits from digital elevation models (DEMs) is the first step in most techniques used to perform DEM characterization, and to describe the general geomorphometry of a surface.

The objective of this manuscript is to study the effect of Gaussian blurring on the extraction of peaks and pits from DEMs. In Section 2, a brief introduction to Gaussian blurring is provided. In Section 3, a mathematical morphological-based algorithm to extract peaks and pits from DEMs is developed. In Section 4, the effect of Gaussian blurring on the extraction of peaks and pits from DEMs is studied. In Section 5, the application of Gaussian blurring to perform DEM smoothing is studied. Concluding remarks and perspectives for further research are presented in Section 6.

## 2. Gaussian blurring

Gaussian blurring is an isotropic smoothing operator that is used to remove the extremities of an image. As shown in Figure 2.1, the kernel used to perform Gaussian blurring, the Gaussian kernel  $G$ , represents a circularly symmetrical bell-shaped hump. The Gaussian kernel is computed using the following function:

$$G(X, Y) = \frac{1}{2\pi\sigma^2} e^{-(x^2+y^2)/2\sigma^2}, \quad (2.1)$$

where  $x$  and  $y$  are Cartesian distances and  $\sigma$  is the standard deviation [2].

This kernel is used as a convoluted point spread function to perform Gaussian blurring. Before performing the convolution operation, a discrete approximation of the Gaussian kernel needs to be computed as the image is stored as a collection of discrete pixels, rather than as a continuous function. Figure 2.2 shows the discrete approximation of the Gaussian kernel shown in Figure 2.1. Using this discrete kernel, Gaussian blurring can be performed using standard convolution methods [2].

## 3. The extraction of peaks and pits from DEMs using ultimate erosion

In this section, an algorithm to extract peaks and pits from DEMs is developed using concepts of mathematical morphology [4–6]. Mathematical morphology deals with the extraction of image components that are useful in representation and description of region shape, such as boundaries, skeletons, and convex hulls [7]. Mathematical morphology is well suited to the processing of elevation data because in morphology, any image is viewed as a topographic surface, the gray level of a pixel standing for its elevation [8]. Hence, mathematical morphological operators are extremely useful and important in DEM analysis. Morphological operators generally require two inputs; the input image  $A$ ,

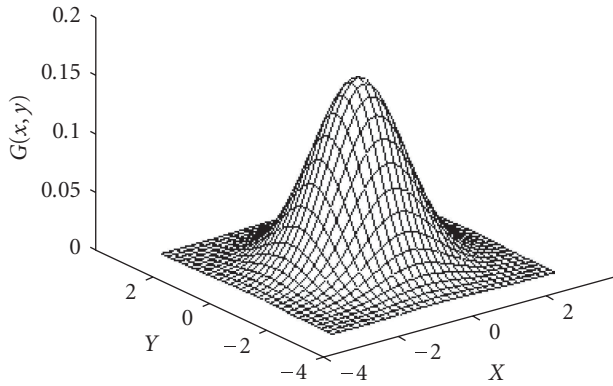


Figure 2.1. A Gaussian kernel, with  $x = 5, y = 5$  and  $\sigma = 1.0$ . (Source: [2])

	1	4	7	4	1
	4	16	26	16	4
1/273	7	26	41	26	7
	4	16	26	16	4
	1	4	7	4	1

Figure 2.2. The discrete approximation of the Gaussian kernel shown in Figure 2.1.

which can be in binary or gray scale form, and the kernel  $B$ , which is used to determine the precise effect of the operator [5].

Dilation sets the pixel values within the kernel to the maximum value of the pixel neighborhood. The dilation operation is expressed as

$$A \oplus B = \{a + b : a \in A, b \in B\}. \tag{3.1}$$

Erosion sets the pixels values within the kernel to the minimum value of the kernel. Erosion is the dual operator of dilation:

$$(A \ominus B) \subset (A^c \oplus B)^c, \tag{3.2}$$

where  $A^c$  denotes the complement of  $A$ , and  $B$  is symmetric with respect to reflection about the origin.

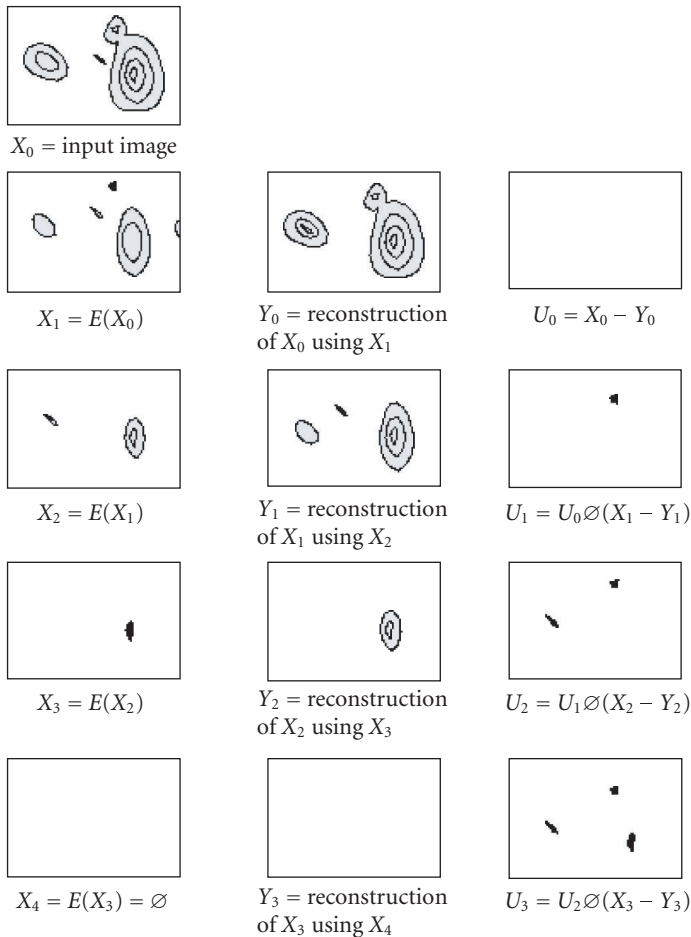


Figure 2.3. An example of the ultimate erosion operation. Ultimate erosion is implemented through the iterative erosion of the image until all objects vanish (images  $X_i$ ), and the reconstruction of each eroded image using the eroded image,  $E(X_i)$ , as the mask and the erosion of smaller size as the marker. The reconstructed images (images  $Y_i$ ) are subtracted from the corresponding eroded images to form the eroded sets (images  $U_i$ ). The final resultant image is known as the ultimate erode set. (Source: [3].) When a particle disappears after an erosion, it is not reconstructed and thus appears in image  $U_i$ .

Gray scale erosion can be used to remove bright areas in gray scale images. It causes small peaks in the image to disappear. However, it also causes valley widening which results in larger peak.

Morphological reconstruction allows for the isolation of certain features within an image based on the manipulation of a mask image  $X$  and a marker image  $Y$ . It is founded on the concept of geodesic transformations, where dilations or erosions of a marker image are performed until stability is achieved (represented by a mask image) [9].

The geodesic dilation,  $\delta^G$ , used in the reconstruction process is performed through iteration of elementary geodesic dilations,  $\delta_{(1)}$ , until stability is achieved,

$$\delta^G(Y) = \delta_{(1)}(Y) \circ \delta_{(1)}(Y) \circ \delta_{(1)}(Y) \dots \text{until stability.} \quad (3.3)$$

The elementary dilation process is performed using a standard dilation of size one followed by an intersection,

$$\delta_{(1)}(Y) = Y \oplus B \cap X. \quad (3.4)$$

The operation in (3.4) is used for elementary dilation in binary reconstruction. In gray scale reconstruction, the intersection in the equation is replaced with a pointwise minimum [9].

Morphological reconstruction can be used to maintain the peak removal effect of erosion while avoiding its valley enlargement effect [9]. The peaks removed by erosion can be obtained by subtracting the reconstructed eroded image from the original image.

In order to extract the peaks of a DEM, ultimate erosion is performed on the DEM. Ultimate erosion is implemented by successively eroding an image until all particles vanish and performing morphological reconstruction on each eroded image into the erosion of smaller size [3]. Figure 2.2 demonstrates the operation of ultimate erosion. The generated ultimate eroded set of the DEM forms the peaks of the DEM. The pits of the DEM are the peaks of the inverted DEM; pit extraction is implemented by performing ultimate erosion on the inverted DEM.

The DEM in Figure 3.1 shows the area of Great Basin, Nev, USA. The area is bounded by latitude  $38^\circ 15'$  to  $42^\circ$  N and longitude  $118^\circ 30'$  to  $115^\circ 30'$  W. The DEM is a global digital elevation model (GTOPO30 DEM) and was downloaded from the USGS GTOPO30 web site (<http://edcwww.cr.usgs.gov/landdaac/gtopo30/gtopo30.html>). GTOPO30 DEMs are available at a global scale, providing a digital representation of the Earth's relief at a 30 arc-seconds sampling interval. The land data used to derive GTOPO30 DEMs are obtained from digital terrain elevation data (DTED), the 1-degree DEM for USA, and the digital chart of the world (DCW). The accuracy of GTOPO30 DEMs varies by location according to the source data. The DTED and the 1-degree dataset have a vertical accuracy of  $\pm 30$  m while the absolute accuracy of the DCW vector dataset is  $\pm 2000$  m horizontal error and  $\pm 650$  vertical error [10].

The proposed peak and pit extraction algorithm is implemented on the DEM of Great Basin. The number of extracted peaks (Figure 3.2(a)) and pits (Figure 3.2(b)) is computed using the connected component labeling algorithm proposed in Pitas [11]. A total of 1,315 peaks and 559 pits are extracted from the DEM. A total of 6,010 pixels (6.60%) are classified as peak pixels, while 1,417 pixels (1.56%) are classified as pit pixels.

In Table 3.1, the study area, the peak regions, and the pit regions are compared in terms of their area, mean elevation, mean gradient, local relief, and relative massiveness.

- (1) *Area*: the area of the region occupied by the area is computed as the aggregate of pixels constituting the object region [11].
- (2) *Mean elevation*: it is computed as the average elevation of the pixels that belong to an object's region. It is interpreted as a measure of the volume of the object per unit area.

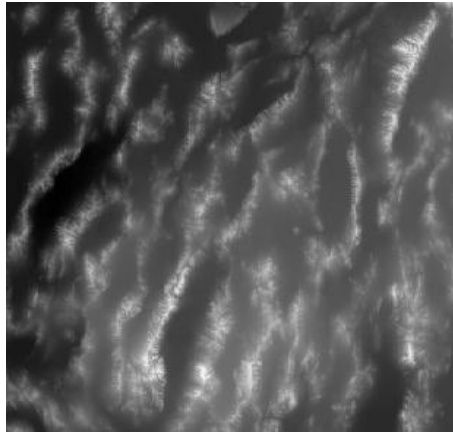


Figure 3.1. The DEM of Great Basin. The elevation values of the terrain (minimum 1005 meters and maximum 3651 meters) were rescaled to the interval of 0 to 255 (the brightest pixel has the highest elevation).

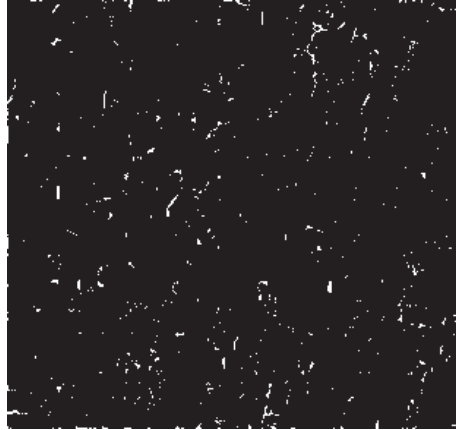
Table 3.1. Statistics of the study area, peak regions, and the pit regions.

Parameter	Study area	Peak regions	Pit regions
Area (pixels)	91123	6010	1417
Mean elevation (gray level)	85.11	127.58	82.64
Mean gradient ( $\circ$ )	5.94	8.95	3.52
Local relief (gray level)	255	249	202
Relative massiveness	0.33	0.49	0.41

- (3) *Mean gradient*: it is computed as the average value of gradient of pixels constituting an object's region.
- (4) *Local relief*: the local relief for a finite area of surface was defined as the difference between the maximum elevation and minimum elevation occurring within that area [12]. It indicates the elevation of a feature from its base.
- (5) *Relative massiveness*: hypsometry is used to study the distributions of elevations across a given area of land. The hypsometric integral (HI) is a process indicator reflecting the stage of landscape development [13] and measuring the extent to which a land surface has been opened up by erosion [12]. More specifically, areas with HI above 0.6 are in the “youthful” stage, areas with HI between 0.35 and 0.6 are in the “equilibrium or mature” stage, and areas with HI below 0.35 are in a transitory “monadnock” stage [13]. From a mathematical point of view, HI equals to the relative massiveness, which is the difference between the mean elevation and the minimum elevation, divided by the local relief. The advantage of relative massiveness is that it is easier to compute. Low relative massiveness values occur in terrain characterized by isolated relief features standing above extensive level surfaces, while high values describe broad, somewhat level surfaces broken by occasional depressions [10].



(a)



(b)

Figure 3.2. Extraction of peaks and pits from the DEM of Great Basin. (a) The extracted peaks. (b) The extracted pits.

#### 4. The effect of Gaussian blurring on the extraction of peaks and pits from DEMs

Gaussian blurring is performed on the DEM of Great Basin using square Gaussian kernels of size 1 to 100 and standard deviation values of 1 to 10. The peaks and the pits of the resultant DEMs are extracted using the proposed peak and pit algorithm. Connected component labeling is used to compute the number of extracted peaks and pits. The results obtained are shown in Figures 4.1 and 4.2.

Gaussian blurring causes the merging of small regions into the surrounding gray level regions, causing removal of fine detail in the DEM. As the Gaussian kernel size and standard deviation are increased, the level of merging increases, resulting in a further loss of fine detail. This causes a reduction in the number of peaks and pits extracted from the

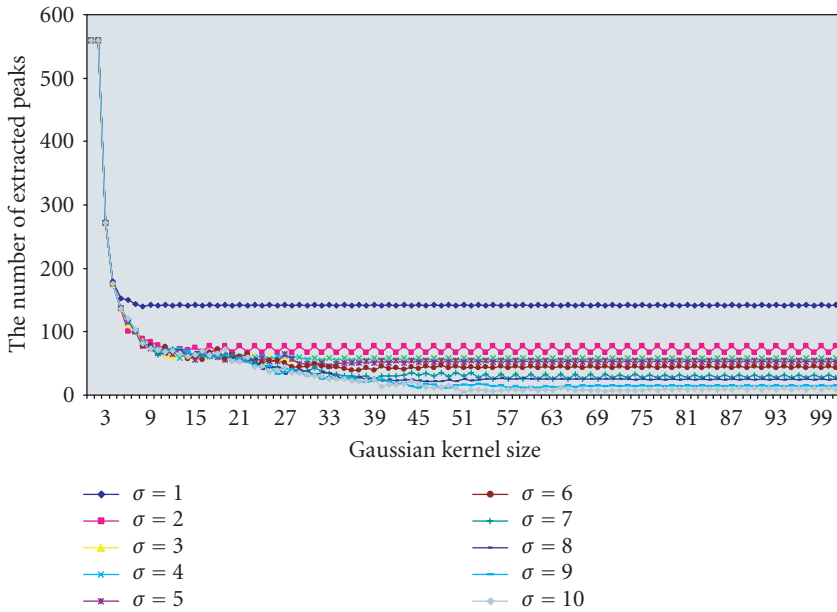


Figure 4.1. The effect of Gaussian blurring on the extraction of peaks from the DEM of Great Basin.

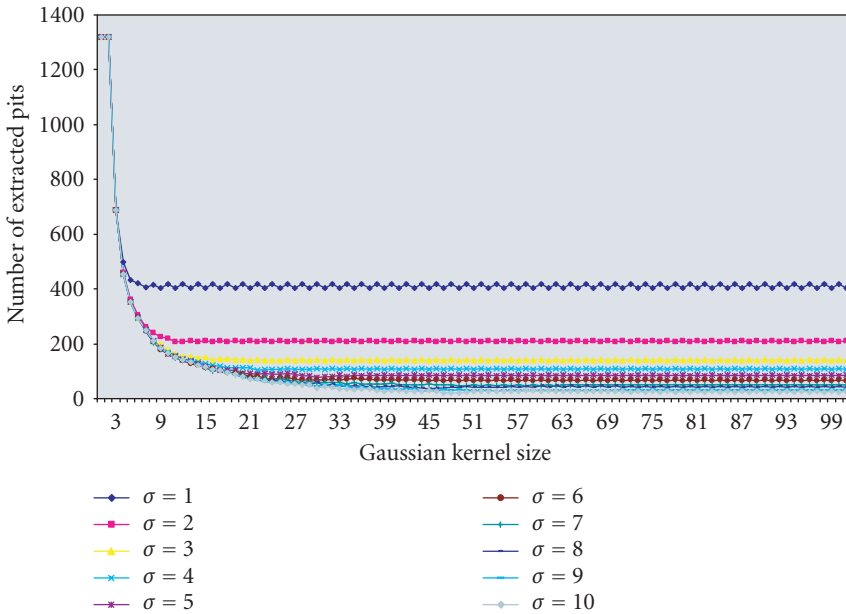


Figure 4.2. The effect of Gaussian blurring on the extraction of pits from the DEM of Great Basin.

DEM. As the Gaussian kernel size is increased, the number of extracted peaks and pits reduces, until a threshold level is reached, whereby an increase in Gaussian kernel size no longer causes major changes in the number of extracted peaks and pits. This threshold level indicates that there the Gaussian kernel can cause no further merging of small regions into their surrounding gray levels. This threshold level is reduced by increasing the standard deviation value of the Gaussian kernel.

## 5. DEM smoothing using Gaussian blurring

This study provides useful insight into the application of Gaussian blurring in the treatment of spurious peaks and pits in DEMs. Spurious peaks and pits are errors that caused input data error, interpolation procedures, and the limited horizontal and vertical resolutions of DEMs. Spurious peaks and pits do not correspond to real landscape features and cause distortions in features extracted from DEMs. Hence, the removal of spurious peaks and pits from DEMs, known as DEM smoothing, is an important preprocessing step in DEM analysis.

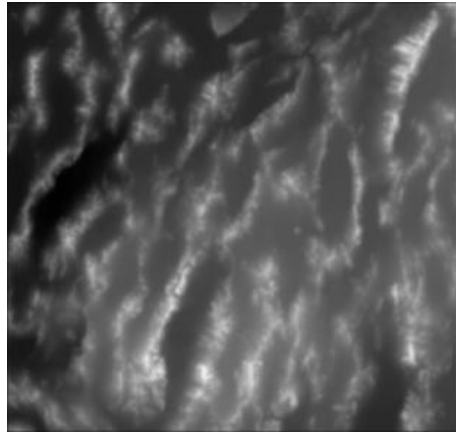
Gaussian blurring is performed on the DEM of Great Basin using a square Gaussian kernel of size 3 ( $\sigma = 1$ ) to obtain a smoothed DEM (Figure 5.1(a)). The mask of pixels modified by Gaussian blurring is shown in Figure 5.1(b). The effectiveness of DEM smoothing using Gaussian blurring is tested by performing drainage network extraction on the original and smoothed DEMs of Great Basin.

The drainage network extraction algorithm used in this paper is the drainage skeletonization algorithm proposed by Meisels et al. [14]. The algorithm extracts pixels that lie in high curvature contours starting from pixels of maximal elevation, elevation-level by elevation-level; the selection is based on a condition for an enough large number of higher elevation pixels in the immediate neighborhood of a pixel belonging to the elevation being processed currently. Complementary local conditions of connectivity are then used to connect all the pixels of the flow path.

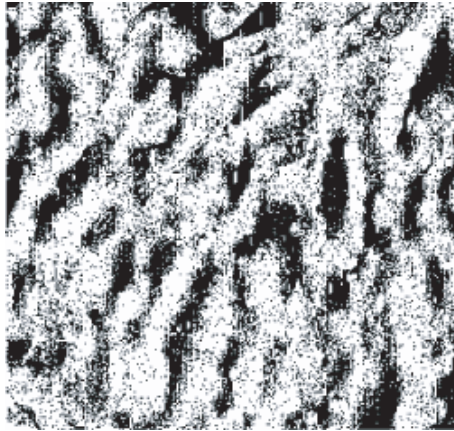
As shown in Figure 5.2(a), spurious peaks in the original DEM cause the formation of closed loops in the extracted drainage network. Spurious pits in the DEM cause a portion of the extracted drainage network to be incomplete and disconnected. As shown in Figure 5.2(b), drainage network extraction applied to the smoothed DEM allows for the extraction of drainage networks that are loopless, complete, and connected.

## 6. Conclusion

In this paper, a geomorphometric case study was employed to demonstrate the capabilities of Gaussian blurring in the modeling of objects and processes operating within an environment; in this case, the peaks and pits of a terrain. Gaussian blurring causes a reduction in the number of peaks and pits extracted from DEMs. As the Gaussian kernel size is increased, the number of extracted peaks and pits reduces, until a threshold level is reached, whereby an increase in Gaussian kernel size no longer causes major changes in the number of extracted peaks and pits. This threshold level is reduced by increasing the standard deviation value of the Gaussian kernel.



(a)

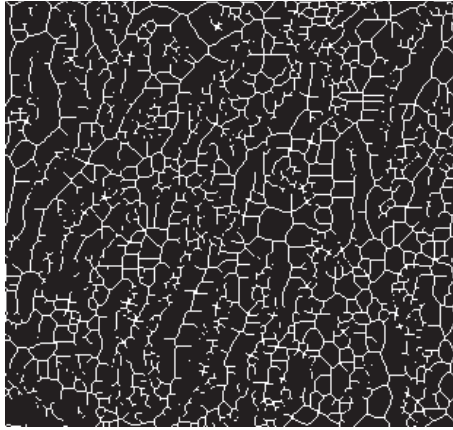


(b)

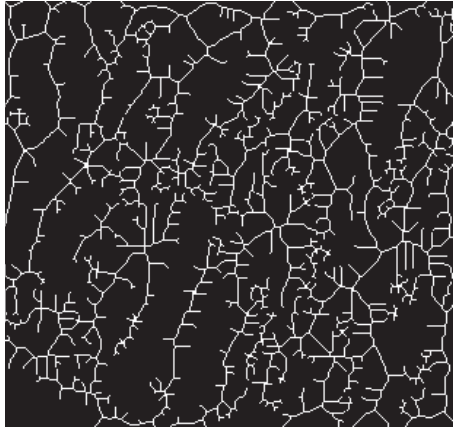
Figure 5.1. DEM smoothing using Gaussian blurring. (a) The smoothed DEM. (b) The mask of pixels modified by Gaussian blurring.

The application of Gaussian blurring to perform DEM smoothing was also demonstrated. Spurious peaks and pits in the original DEM of Great Basin cause the extracted drainage network to be incomplete and disconnected and to contain closed loops. The drainage network of smoothed DEM is loopless, complete, and connected.

Gaussian blurring is the first step in the extraction of various geomorphological features, such as watersheds [15] and mountains [15, 16]. In general, it is observed that in terrain modeling, Gaussian blurring causes the change in variation of spatial extent in a time sequential mode. Analysis of a feature at varying scales over a duration of time allows



(a)



(b)

Figure 5.2. Extraction of drainage networks from the original and smoothed DEMs of Great Basin. (a) The drainage network extracted from original DEM. (b) The drainage network extracted from the smoothed DEM.

for a greater amount of information to be extracted about the spatiotemporal characteristics of the feature. At present, work is being carried out to perform the modeling of the spatiotemporal organization of watersheds and mountains using Gaussian blurring.

### **Acknowledgment**

The authors are grateful to Associate Professor Behara Seshadri Daya Sagar of the Faculty of Engineering and Technology, Multimedia University, for his valuable comments and guidance.

## References

- [1] United States Geological Survey (USGS), *Digital Elevation Models: Data Users Guide 5*, 1987, US Department of the Interior, Reston, Va, USA.
- [2] B. Fisher, S. Perkins, A. Walker, and E. Wolfart, *Hypermedia Image Processing Reference*, John Wiley & Sons, New York, NY, USA, 1994.
- [3] P. Duchene and D. Lewis, "Visilog 5 Documentation," Noesis Vision, Quebec, Canada, 1996.
- [4] G. Matheron, *Random Sets and Integral Geometry*, John Wiley & Sons, New York, NY, USA, 1975.
- [5] J. Serra, *Image Analysis and Mathematical Morphology*, Academic Press, London, UK, 1982.
- [6] P. Soille, *Morphological Image Analysis: Principles and Applications*, Springer, Berlin, Germany, 2nd edition, 2003.
- [7] R. C. Gonzalez and R. E. Woods, *Digital Image Processing*, Addison-Wesley, New York, NY, USA, 1993.
- [8] P. Arrighi and P. Soille, "From scanned topographic maps to digital elevation models," in *Proceedings of International Symposium on Imaging Applications in Geology (GeoVision '99)*, pp. 1–4, University of Liege, Liege, Belgium, 1999.
- [9] L. Vincent, "Morphological grayscale reconstruction in image analysis: applications and efficient algorithms," *IEEE Transactions on Image Processing*, vol. 2, no. 2, pp. 176–201, 1993.
- [10] G. Ch. Miliareisis and D. P. Argialas, "Quantitative representation of mountain objects extracted from the global digital elevation model (GTOPO30)," *International Journal of Remote Sensing*, vol. 23, no. 5, pp. 949–964, 2002.
- [11] I. Pitas, *Digital Image Processing Algorithms*, Prentice Hall International Series in Acoustics, Speech and Signal Processing, Prentice-Hall, Englewood Cliffs, NJ, USA, 1993.
- [12] D. M. Mark, "Geomorphometric parameters: a review and evaluation," *Geografiska Annaler*, vol. 57, no. 3-4, pp. 165–177, 1975.
- [13] A. N. Strahler, "Hypsometric (area-altitude curve) analysis of erosional topography," *Bulletin of the Geological Society of America*, vol. 63, no. 11, pp. 1117–1142, 1952.
- [14] A. Meisels, S. Raizman, and A. Karnieli, "Skeletonizing a DEM into a drainage network," *Computers & Geosciences*, vol. 21, no. 1, pp. 187–196, 1995.
- [15] S. Dinesh, "Extraction of hydrogeomorphic features from digital elevation models using mathematical morphology," M.S. thesis, Multimedia University, Melaka, Malaysia, 2006.
- [16] S. Dinesh, P. Radhakrishnan, and B. S. D. Sagar, "Morphological segmentation of physiographic features from DEM," to appear in *International Journal of Remote Sensing*.

A. Pathmanabhan: Faculty of Engineering and Technology, Multimedia University,  
Jalan Air Keroh Lama, Melaka 75450, Malaysia  
Email address: pathma\_hans@hotmail.com

S. Dinesh: Science and Technology Research Institute for Defence (STRIDE), Ministry of Defence,  
Bahagian Teknologi Maritim, D/A KD Malaya, Pangkalan TLDM, Perak 32100, Lumut, Malaysia  
Email address: dinsat@yahoo.com



# Hindawi

Submit your manuscripts at  
<http://www.hindawi.com>

